Ultracompact nonreciprocal optical isolator based on guided resonance in a magneto-optical photonic crystal slab

Kejie Fang,[1,3] Zongfu Yu,[2] Victor Liu,[2] and Shanhui Fan[2,4]

[1]*Department of Physics, Stanford University, 382 Via Pueblo Mall, Stanford, California 94305, USA*

[2]*Ginzton Laboratory, Stanford University, 450 Via Palou Mall, Stanford, California 94305, USA*

[3]*e-mail: kfang@stanford.edu*

[4]*e-mail: shanhui@stanford.edu*

Received June 28, 2011; revised August 16, 2011; accepted September 29, 2011;
posted September 30, 2011 (Doc. ID 150033); published October 28, 2011

We design an ultracompact optical isolator with normal incident geometry that operates with a bandwidth that is substantial for a device of this size. For operation in a telecommunication wavelength of 1.55 μm, the thickness of the device is less than 1 μm and the device supports an operating bandwidth of 400 GHz over which the minimum contrast ratio exceeds 25 dB. Our design utilizes guided resonance in a photonic crystal slab to enhance magneto-optical effects, and exploits interference effects among multiple resonances to create desired transmission spectral line shapes.

OCIS codes: 230.3240, 160.3820.

Traditional magneto-optical devices, such as Faraday rotators, have a large length typically of the scale of 10^{-2}–10^{-3} m, since the magneto-optical effect in a transparent medium is typically weak. The goal to miniaturize magneto-optical devices has motivated the use of optical resonances to enhance magneto-optical effects. Examples include various device configurations in one-dimensional magneto-optical photonic crystals [1–6], on-chip circulators in two-dimensional photonic crystals [7–9], and on-chip isolators based on ring resonators [10,11].

Here we propose a guided-resonance-based [12] magneto-optical isolator that exhibits a nonreciprocal transmission effect over a substantial bandwidth. The device consists of a photonic crystal slab made from magneto-optical materials, with a periodic array of air holes introduced into the slab (Fig. 1). Light is normally incident onto the slab. In terms of operating configuration, this device is similar to previous works on resonators in one-dimensional magneto-optical photonic crystals [1–4], in that light is coupled in from free space in the vertical direction. However, in a one-dimensional magneto-optical photonic crystal, strong resonance effects are achieved with the use of a large number (typically more than 10) of alternating dielectric layers, whereas, in this design, a single layer is sufficient. Also related to this work, [13–15] discussed nonreciprocal transmission through a perforated metal film coupled to a magneto-optical material. Our work differs in that we do not utilize any metallic element that is lossy and, therefore, our structures should, in principle, have lower intrinsic loss.

In the photonic crystal slab structure in Fig. 1, we assume that the magneto-optical material is bismuth iron garnet (BIG), which has a permittivity tensor

$$\epsilon = \begin{pmatrix} \epsilon_r & i\epsilon_i & 0 \\ -i\epsilon_i & \epsilon_r & 0 \\ 0 & 0 & \epsilon_r \end{pmatrix}, \qquad (1)$$

with $\epsilon_r = 6.25$, $\epsilon_i = 0.06$ at saturation at the wavelength of 1.55 μm, when the magnetization is along the $+z$ direction [16,17]. The photonic crystal slab has a square lattice with lattice constant a and thickness $d = 0.5a$ (Fig. 1). In each unit cell, there is one square air hole in the center with full side length $b_1 = 0.4a$, and four square air holes at the corners with full side length $b_2 = 0.18a$. Here, the entire structure is of a single magnetic domain. The corner air holes are introduced to maximize the magneto-optical effect for such a single domain structure.

The photonic crystal slab made of magneto-optical material in Fig. 1 has C_4 symmetry, which includes rotations of 0°, 90°, 180°, and 270° around the z axis. At normal incidence, the two circular polarizations belong to two different one-dimensional representations of C_4, and thus they do not mix. As a result, for a circularly polarized plane wave normally incident on the photonic crystal slab in Fig. 1, the transmitted wave is still circularly polarized with the same chirality.

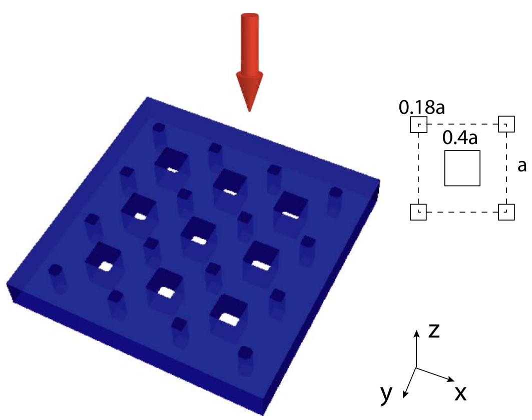

Fig. 1. (Color online) Photonic crystal slab consisting of magneto-optic material and air holes. The lattice constant is a and the thickness of the slab is $d = 0.5a$. The side lengths of the large and small air holes in the unit cell are $b_1 = 0.4a$ and $b_2 = 0.18a$, respectively. Top right is the top view of the unit cell (dashed line). The origin of the coordinates is at the center of the larger air hole in the middle of the slab. The arrow denotes the normally incident light.

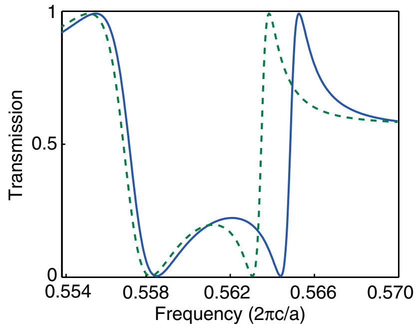

Fig. 2. (Color online) Intensity transmission spectra for normally incident left circularly polarized (green dashed) and right circularly polarized (blue) light from top through the photonic crystal slab in Fig. 1.

For the two circular polarizations, the transmission spectra for plane waves incident from above the structure are calculated using rigorous coupled wave analysis [18], and are shown in Fig. 2. The total number of plane waves used in the numerical calculation is 385 [19].

For each transmission spectrum plotted in the chosen frequency range, there are two Fano resonances [12] corresponding to the first TE-like and TM-like guided resonance in the photonic crystal slab, respectively. The field distributions of these two resonances are shown in Fig. 3. The transverse components of the electric field of TE-like and TM-like resonances have even and odd symmetry with respect to the center ($z = 0$ plane) of the slab. The TM-like resonance has a narrower linewidth, consistent with previous studies [20].

We observe that the transmission spectra split for the two circular polarizations. The origin of this split can be understood by considering a corresponding nonmagnetic system that is the same as Fig. 1, except that ϵ_i in Eq. (1) is set to zero. Such a nonmagnetic system has its symmetry described by a C_{4v} group, which includes, in addition to the 90° rotation, mirror operations with respect to the x-normal and y-normal mirror planes. The C_{4v} group supports an irreducible two-dimensional representation and hence the structure has resonances that are twofold degenerate. Such twofold degenerate resonances are the only resonances that can couple to normally incident plane waves [12]. When $\epsilon_i \neq 0$, the degeneracy is lifted by the magneto-optical effect, and each of the two split resonances couples to only one of the two circular polarizations. As a result, the transmission spectra of the two circular polarizations also split, as we see in Fig. 2.

The split in resonant frequency can be estimated using perturbation theory [7]:

$$\Delta\omega = \frac{\omega_0 \int dV \epsilon_i \hat{\vec{z}} \cdot (\vec{E}_1^* \times \vec{E}_2)}{\sqrt{\int dV \epsilon_r |\vec{E}_1|^2 \int dV \epsilon_r |\vec{E}_2|^2}}, \tag{2}$$

where $\vec{E}_1$ and $\vec{E}_2$ are the electric fields of the two degenerate resonances and ω_0 is the resonant frequency, all for the corresponding nonmagnetic system. Note the integrand in the numerator of Eq. (2) generally changes sign in the unit cell [7]. In our design, the positions and sizes of the air holes are chosen such that, within the magneto-optical materials, the integrand in Eq. (2) is of the same sign, in order to maximize the frequency splitting $\Delta\omega$.

We observe that, in Fig. 2, between the two circular polarizations, the TM-like resonances have a larger frequency split compared with the TE-like resonances. This may seem surprising, since, as seen in Eq. (2), the contribution to the frequency splitting is solely from the in-plane components of the electric fields. At the mirror plane normal to the z direction at the center of the structure, the TM-like resonance has no in-plane electric fields. However, the in-plane electric field of the TM-like resonance near the surface of the slab is in fact substantial, and as a result, the TM-like resonance can have substantial magneto-optical activity. For a more detailed examination, in Fig. 4 we consider the corresponding nonmagnetic structure, and plot the E_y field of one of the TE-like resonances in the center x–y plane of the slab ($z = 0$), and the E_y field of one of the TM-like resonances at $z = 0.2a$. These two planes are located where the in-plane electric fields are maximum for the two sets of resonances, respectively. The resonances are excited by a normally incident light with linear polarization in the y direction. The field of the other degenerate mode can be obtained by a 90° rotation. As can be seen from Fig. 4, for the TE-like resonance, E_y is primarily distributed in the air holes where there is no contribution to the magneto-optical effect. On the other hand, for the TM-like resonance, E_y is primarily outside the holes in the dielectric region. Thus, in the presence of a nonzero ϵ_i, the TM-like resonance in fact exhibits a stronger magneto-optical effect. Starting from the field pattern of the corresponding nonmagnetic structure, and using Eq. (2), we calculate, for the magnetic structure, the frequency split between the two polarizations. The split for TE-like

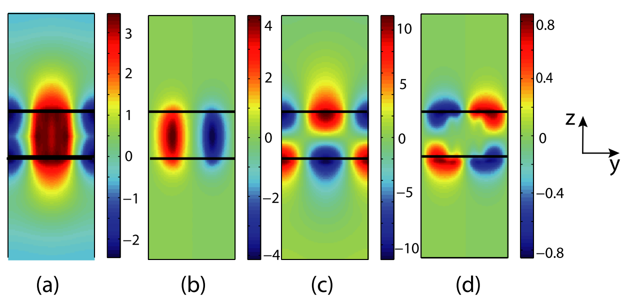

Fig. 3. (Color online) x and y components of the electric field of the guided resonances in a vertical plane at $y = 0.25a$. (a) and (b) are the E_x and E_y field components of the TE-like resonance. (c) and (d) are the E_x and E_y field components of the TM-like resonance. The solid lines indicate the top and bottom surfaces of the slab.

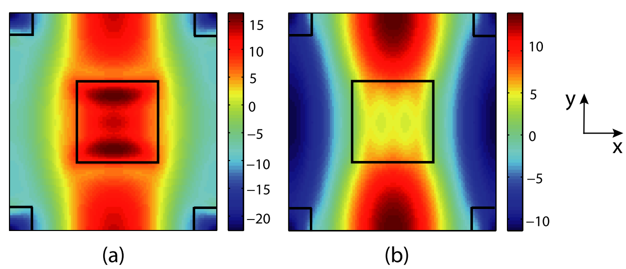

Fig. 4. (Color online) E_y field of the guided resonances. (a) E_y of TE-like resonance in the center of the slab ($z = 0$) and (b) E_y of TM-like resonance in a plane with $z = 0.2a$. The regions enclosed by the solid lines represent the air holes. The field is excited by linearly polarized light with only an E_y component.

and TM-like resonance is $2.26 \times 10^{-4}(2\pi c/a)$ and $1.23 \times 10^{-3}(2\pi c/a)$, respectively, in agreement with the split of $2.80 \times 10^{-4}(2\pi c/a)$ for TE-like resonance and $1.32 \times 10^{-3}(2\pi c/a)$ for TM-like resonance, as determined from the transmission spectra in Fig. 2.

The slab structure considered here is nonreciprocal. For circularly polarized plane waves, the time-reversal operation reverses the propagation direction while preserving the handedness of the polarization. Hence, to see the nonreciprocity, we need to show that, for left circularly polarized light, the transmission spectra are different when it is incident from above and below the slab. On the other hand, our structure has a mirror symmetry with respect to the mirror plane normal to the z direction. (The magnetization vector is a pseudovector and thus does not change direction under the mirror operation.) The mirror operation reverses both the propagation direction and the handedness of a circularly polarized plane wave. Because of such mirror symmetry, for our structure the transmission coefficient of a left circularly polarized light incident from below the slab is equal to that of a right circularly polarized light incident from above. As a result, the difference that we see in the transmission spectra for light incident from above the slab, between the two circular polarizations, in fact indicates the contrast between two scenarios that are related by the time-reversal operation, and hence proves the nonreciprocity of the device. The operation of the structure is intrinsically different from reciprocal chiral structures that, as a matter of principle, cannot provide complete optical isolation.

The spectra in Fig. 2 are for incident plane waves. For a finite incident beam, suppose we operate at the wavelength of 1.55 μm, where the left circularly polarized plane wave reaches a transmission maximum of 100% at normal incidence (Fig. 2). A normally incident Gaussian beam with the same polarization, and with a beam size of 28 μm, will have a power transmission coefficient of 99.6%.

The discussion above indicates some of the general considerations in using guided resonances to achieve a strong nonreciprocal response. The multiresonance interference effect in these systems provides further opportunities to enlarge the operating bandwidth and enhance the contrast ratio. In our structure, the TE-like and TM-like guided resonances have opposite symmetry with respect to the mirror plane normal to the z direction. The transmission spectrum of the structure depends strongly on the frequency difference between these two classes of resonances with opposite symmetry [21,22]. As an illustration, we consider the same structure as shown in Fig. 1, except we enlarge the corner air hole to a side length of $0.1984a$. In this case, the right circularly polarized light exhibits a flattop line shape, since its TE-like and TM-like resonances have a frequency splitting that is comparable to the linewidth [22], whereas the left circularly polarized light has a transmission peak (Fig. 5). As a result, the structure, operating at a wavelength of 1.55 μm, exhibits a bandwidth of 400 GHz with a contrast ratio between the two circular polarizations above 25 dB. The thickness of the device is only 0.87 μm. A thin etched BIG film could have nonuniformity due to the granularity [23]. Thus, the specific operation frequency could be affected. However, the isolation due to the split of the resonance frequencies is robust.

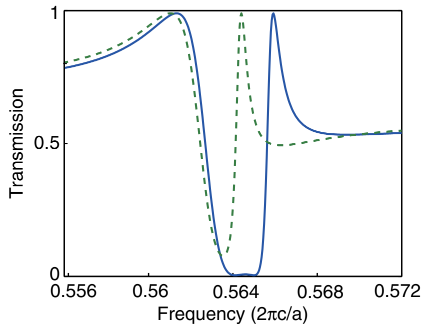

Fig. 5. (Color online) Intensity transmission spectra for the normally incident left circularly polarized (green dashed) and right circularly polarized (blue) light through a photonic crystal slab. The slab is the same as in Fig. 1, except that the corner air hole now has a side length of $b_2 = 0.1984a$. For an operation wavelength of 1.55 μm, the lattice constant $a = 1.74\,\mu$m and the thickness of the slab $d = 0.87\,\mu$m.

This work is supported in part by U. S. Air Force Office of Scientific Research (USAFOSR, FA9550-09-1-0704), and by the National Science Foundation (NSF, Grant No. DMS-0968809).

References and Notes

1. M. Inoue, K. Arai, T. Fujii, and M. Abe, J. Appl. Phys. **83**, 6768 (1998).
2. S. Sakaguchi and N. Sugimoto, Opt. Commun. **162**, 64 (1999).
3. M. J. Steel, M. Levy, and R. M. Osgood, IEEE Photon. Technol. Lett. **12**, 1171 (2000).
4. M. J. Steel, M. Levy, and R. M. Osgood, J. Lightwave Technol. **18**, 1297 (2000).
5. R. Li and M. Levy, Appl. Phys. Lett. **86**, 251102 (2005).
6. Z. Yu, Z. Wang, and S. Fan, Appl. Phys. Lett. **90**, 121133 (2007).
7. Z. Wang and S. Fan, Appl. Phys. B **81**, 369 (2005).
8. Z. Wang and S. Fan, Opt. Lett. **30**, 1989 (2005).
9. W. Smigaj, J. Romero-Vivas, B. Gralak, L. Magdenko, B. Dagens, and M. Vanwolleghem, Opt. Lett. **35**, 568 (2010).
10. N. Kono, K. Kakihara, K. Saitoh, and M. Koshiba, Opt. Express **15**, 7737 (2007).
11. M.-C. Tien, T. Mizumoto, P. Pintus, H. Kroemer, and J. E. Bowers, Opt. Express **19**, 11740 (2011).
12. S. Fan and J. Joannopoulos, Phys. Rev. B **65**, 235112 (2002).
13. V. I. Belotelov, D. A. Bykov, L. L. Doskolovich, A. N. Kalish, and A. K. Zvezdin, J. Opt. Soc. Am. B **26**, 1594 (2009).
14. A. B. Khanikaev, S. H. Mousavi, G. Shvets, and Y. S. Kivshar, Phys. Rev. Lett. **105**, 126804 (2010).
15. H. Zhu and C. Jiang, Opt. Lett. **36**, 1308 (2011).
16. N. Adachi, V. P. Denysenkov, S. I. Khartsev, and A. M. Grishin, J. Appl. Phys. **88**, 2734 (2000).
17. T. Tepper and C. A. Ross, J. Cryst. Growth **255**, 324 (2003).
18. D. M. Whittaker and I. S. Culshaw, Phys. Rev. B **60**, 2610 (1999).
19. The relative variation of resonance frequency when the number of plane waves is 889 is less than 0.2%.
20. M. Beheiry, V. Liu, S. Fan, and O. Levi, Opt. Express **18**, 22702 (2010).
21. W. Suh, Z. Wang, and S. Fan, IEEE J. Quantum Electron. **40**, 1511 (2004).
22. W. Suh and S. Fan, Appl. Phys. Lett. **84**, 4905 (2004).
23. S. Kahl, "Bismuth iron garnet films for magneto-optical photonic crystals," Ph.D. dissertation (Department of Condensed Matter Physics/KTH, Royal Institute of Technology, Stockholm, Sweden, 2004).